Supplemental Materials

Systematic investigation of recipient cell genetic requirements reveals important surface receptors for conjugative transfer of IncI2 plasmids

Nancy Allard[1], Arianne Collette[1], Josianne Paquette[1], Sébastien Rodrigue[1]* and Jean-Philippe Côté[1*]

[1] Département de biologie, Faculté des sciences, Université de Sherbrooke, Sherbrooke, QC J1K 2R1, Canada

* Correspondence may be addressed to:

Sébastien Rodrigue
Tel: 1-819-821-8000 ext. 62939
Email : Sebastien.Rodrigue@USherbrooke.ca

Jean-Philippe Côté
Tel :1-819-821-8000 ext. 65280
Email : JP.Cote@USherbrooke.ca

This Supplemental Material includes:

Supplementary discussion

Supplementary Tables 1 to 2

Supplementary Figures 1 to 8

Supplementary References

Supplementary discussion

LPS structure description

The outer membrane of Gram-negative bacteria is an essential feature acting like a barrier to protect cells from toxic compounds such as antibiotics and detergents[1]. From the outer membrane to the extracellular space, the LPS structure consists of (i) lipid A, a hydrophobic glycolipid which anchors LPS in the outer membrane; (ii) core oligosaccharide (core-OS), a non-repeating oligosaccharide containing sugars such as heptose and keto-deoxyoctulosonate (Kdo); and (iii) O antigen, a polysaccharide made of up to 50 repeating oligosaccharide subunits (Fig. 3 c). LPS biosynthesis involves a large number of enzyme activities, governed by more than 40 genes[2,3] that account for a large structural diversity. In the *Enterobacteriaceae*, the core-OS is divided into two distinct regions, the inner and the outer core-OS (Fig. 3 c). The inner core is highly conserved and comprises three Kdo and L-*glycero*-D-*manno*-heptose (Hep) residues and is often phosphorylated. The outer core-OS comprises a tri-hexose backbone that can be modified with varying side-branch substitutions[4]. *Escherichia coli* serotypes are determined by the type of polysaccharide antigens on their cell membrane including the O antigen. A total of ~178 distinct antigens have been formally defined for *E. coli* alone. This diversity allows bacteria to have a surface that offers a selective advantage in its specific niche[3]. Despite this high degree of diversity in O antigen, only five distinct core-OS structures are found in *E. coli*, designated K-12, R1, R2, R3 and R4 (Fig. 5 b). These core-OS structures are synthesized through the successive addition of various sugars to lipid A by the products of the *waa* genes (formerly *rfa* genes)[4].

PilV variants recognize receptor structures in the core-OS of *E. coli* LPS

The loss of long O16 antigen in *E. coli* BW25113 (K-12 core-oligosaccharide) is due to the disruption of the rhamnosyl transferase *wbbL* gene with an IS5 element, termed the *rfb-50* mutation[1,5]. Since the complementation of this lesion by insertion of an intact *wbbL* gene from an O antigen-expressing strain of *E. coli* into the

chromosome of *E. coli* BW25113 restored O antigen expression[1,6], all other genes are functional. To ensure that these other genes do not incorporate new sugars into the LPS structure, we generated an *E. coli* BW25113 mutant in which the *rfbABCD*, *wzxB*, *glf* and *wbbHIJKL* genes were removed (Fig. 3 c). This ΔO antigen mutant, exhibiting a core-OS, as well as a mutant displaying only the lipid IVA, called ClearColi[7] (Fig. 3 c), were subjected to pairwise conjugation in broth using all TP114 derivatives bearing a single PilV variant[8] (Fig. 3 d). As previously reported[8], transfer rates of TP114 mutant in which the variable region of *pilV* was replaced by a FLAG tag was virtually unaffected on solid medium, but its capacity to conjugate in broth was severely altered. Moreover, since *E. coli* BW25113 and BW25113ΔO antigen were recognized by the same three adhesins (PilVA', PilVC and PilVC') while ClearColi did not generate any transconjugants, we can infer that these adhesins -and potentially those that did not recognize the K-12 core structure- exhibit specificities for a receptor present in the core-OS.

Elucidation of receptor structure(s) for PilV variants using knockout mutants

Results surrounding the elucidation of receptor structures of PilVA' and PilVC are described in detail in the main article and will not be elaborated here. The use of a donor strain expressing only one PilV variant at a time[8] allowed us to study their specificities towards different recipient bacteria. The pairwise mating experiments in broth allowed us to validate receptor structures since strains displaying the receptor structure at the surface of the cell generated transconjugants, while those missing the receptor molecule do not. For example, the PilVA adhesin of plasmid R64 was shown to specifically bind to *N*-acetylglucosamine-β-(1-3)-glucose[9] (Fig. 5 b). This receptor structure is only present in *E. coli* R1 and thus this strain is the only one producing transconjugants when mating with TP114-bearing PilVA adhesin, which is homologous to R64 PilVA. Moreover, it was shown that a Δ*waaL* knockout mutant of *E. coli* R1 was no longer recognized by PilVA adhesin[9]. Consequently, we expect that cloning the genes responsible for the addition of *N*-acetylglucosamine-β-(1-3)-glucose disaccharide and their expression in a strain

representing one of the other core-OS would produce transconjugants when mating with a donor expressing PilVA adhesin.

The conjugation results with the PilVC' variant were also in agreement with the receptor structure proposed for the homolog of R64 as being glucose-α-(1-2)-glucose or glucose-α-(1-2)-galactose. Indeed, in the case of *E. coli* R2 and *E. coli* BW25113 which displays the K-12 core-OS, the glucose-α-(1-2)-glucose is the target of PilVC' adhesin. Effectively, *E. coli* BW25113Δ*waaR*, missing the third glucose, is no longer recognized by PilVC' adhesin (Supp. Fig. 4 b). Moreover, all other knockout mutants affecting the core-OS lower in the structure, such as Δ*waaO* (Supp. Fig. 4 c), Δ*waaG*, Δ*waaF*, Δ*waaC* (Fig. 4 f, g, h) does not generate transconjugants when mating in broth with a donor harbouring the PilVC' adhesin (Fig. 5 a). On the other hand, in *E. coli* R1 and R4, it is the glucose-α-(1-2)-galactose that acts as a receptor structure (Fig. 5). One intriguing thing about those receptors is that both can be found in the outer core-OS of *E. coli* R3, but this strain does not produce any transconjugants when using the PilVC' adhesin. This could mean that the glucose added by WaaG may be important in the receptor structure. To investigate this possibility, the *waaO* and *waaR* genes could be introduced *in trans* in *E. coli* BW25113 Δ*waaG*. If this strain, harbouring a chimeric LPS, is still recognized by the PilVC' adhesin, then the receptor is a disaccharide, but if not, the receptor could be a trisaccharide.

Elucidation of receptor structure(s) for PilV variants using knock-in mutants

To explore other potential receptor structures, we cloned one or two *waa* genes originating from another core-OS prototype in an arabinose inducible plasmid (pBAD30). For example, when introducing pWaaOX (bearing *waaO* and *waaX* genes from *E. coli* R4) in *E. coli* R3, this new strain expressing chimeric LPS produced transconjugants when mating in broth with the PilVC' adhesin, which was not the case with the wild type strain (Supp. Fig. 4 d, e). Since *waaO* and *waaX* genes are responsible for the incorporation of the galactose-β-(1-4)-glucose in the LPS, this disaccharide is likely a new receptor structure of PilVC' adhesin.

In our results, only the R2 core LPS and strains in which we added the appropriate genes were recognized by the PilVB variant. More precisely, when introducing *waaK in trans* in *E. coli* BW25113 or *waaK* along with *waaR* genes in *E. coli* R4 (Supp. Fig. 4 f, g, h), those strains produced transconjugants when mating in broth with a donor strain harbouring PilVB adhesin, while the wild type strains did not (Supp. Fig. 7). Since *waaK* is responsible for the addition of an *N*-acetylglucosamine sugar on a glucose molecule with an α-(1-2) linker, this modification could occur on the first glucose of BW25113 LPS, thus allowing transconjugants to form upon mating assays in broth using the PilVB adhesin (Fig. 4). This again highlights the fact that the nature of the linker between the two molecules is crucial since there is already an *N*-acetylglucosamine-α-(1-6)-glucose in the O16 antigen of *E. coli* BW25113[5], but the PilVB adhesin does not recognize the wild-type strain. *N*-acetylglucosamine-α-(1-2)-glucose structure was previously proposed as the target of PilVB' for R64[10]. However, our results show that *N*-acetylglucosamine-α-(1-2)-glucose is rather the receptor structure for the PilVB variant.

The introduction of pWaaD, pWaaT, pWaaV, pWaaW, pWaaJ, pWaaVL, pWaaRK, pWaaTW-R1 or pWaaTW-R4 into *E. coli* BW25113 and expression of chimeric LPS did not change the pattern of PilV adhesin recognition of the strains (Supp. Fig. 7).

Supplementary Table 1. Strains and plasmids used in this study.

Strain or plasmid	Description[a]	Source (reference)
Escherichia coli		
EC100D*pir*+	F- *mcrA* ∆(*mrr-hsdRMS-mcrBC*) ϕ80*dlacZ*∆*M15* ∆*lacX74 recA1 endA1 araD139* ∆(*ara, leu*)*7697 galU galK* λ– *rpsL nupG pir*+ (DHFR)	#ECP09500 (Lucigen)
Nissle 1917	Wild type probiotic strain	Brady *et al.* 2013 [11]
KN01∆*dapA*	Nissle 1917∆*dapA*, Sp^R, Sm^R	Neil *et al.* 2020 [12]
VB111	MG1655Nx^R , K-12 F- λ- *ilvG– rfb-50 rph-1*	Ceccarelli *et al.* 2008 [13]
BW25113	F- ∆(*araD-araB*)*567*, ∆*lacZ4787*(::*rrnB-3*), λ-, *rph-1*, ∆(*rhaD-rhaB*)*568*, *hsdR514*	CGSC #7636
BW25113∆O antigen::Kn^R	BW25113 where O antigen (*rfbABCD*, *wzxB*, *glf*, *wbbHIJKL*) have been replace by Kn^R by recombineering	This study
BW25113∆*waaB*::Kn^R	Keio mutant JW3603	Baba *et al.* 2006 [14]
BW25113∆*waaC*::Kn^R	Keio mutant JW3596	Baba *et al.* 2006 [14]
BW25113∆*waaE*::Kn^R	Keio mutant JW3024	Baba *et al.* 2006 [14]
BW25113∆*waaF*::Kn^R	Keio mutant JW3595	Baba *et al.* 2006 [14]
BW25113∆*waaG*::Kn^R	Keio mutant JW3606	Baba *et al.* 2006 [14]
BW25113∆*waaL*::Kn^R	Keio mutant JW3597	Baba *et al.* 2006 [14]
BW25113∆*waaO*::Kn^R	Keio mutant JW3602	Baba *et al.* 2006 [14]
BW25113∆*waaP*::Kn^R	Keio mutant JW3605	Baba *et al.* 2006 [14]
BW25113∆*waaQ*::Kn^R	Keio mutant JW3607	Baba *et al.* 2006 [14]
BW25113∆*waaR*::Kn^R	Keio mutant JW3601	Baba *et al.* 2006 [14]
BW25113∆*waaS*::Kn^R	Keio mutant JW3604	Baba *et al.* 2006 [14]
BW25113∆*waaY*::Kn^R	Keio mutant JW3600	Baba *et al.* 2006 [14]
BW25113∆*waaZ*::Kn^R	Keio mutant JW3599	Baba *et al.* 2006 [14]
BW25113∆*gmhB*::Kn^R	Keio mutant JW0196	Baba *et al.* 2006 [14]
BW25113∆*gmhD*::Kn^R	Keio mutant JW3594	Baba *et al.* 2006 [14]

Supplementary Table 1. Strains and plasmids used in this study (continued).

Strain or plasmid	Description[a]	Source (reference)
BW25113Δ*hlyT*::Kn^R	Keio mutant JW3818	Baba *et al.* 2006 [14]
BW25113Δ*kdsC*::Kn^R	Keio mutant JW3165	Baba *et al.* 2006 [14]
F470†	Standard for R1 prototype O-:K-, R-LPS mutant of O8:K27	Tsang *et al.* 1987 [15]
F632†	Standard for R2 prototype O-:K-, R-LPS mutant of O100	Tsang *et al.* 1987 [15], Hämmerling *et al.* 1971 [16]
F653†	Standard for R3 prototype O-:K-, R-LPS mutant of O111:K58	Tsang *et al.* 1987 [15]
F2513†	Standard for R4 prototype O-:K-, R-LPS mutant of O14:K7	Tsang *et al.* 1987 [15]
ClearColi	BL21(DE3) *msbA148* Δ*gutQ* Δ*kdsD* Δ*lpxLMP* Δ*pagP* Δ*eptA*	Mamat *et al.* 2013 [7]
Plasmid		
pBAD30	*oriV*$_{p15A}$, *bla* (Ap^R), *araC*, P$_{BAD}$	Guzman *et al.* 1995 [17]
pE-FLP	*oriV*$_{pSC101ts}$, *flp*, *bla* (Ap^R)	Addgene #45978
pKD3	*oriV*$_{R6K}$, FRT flanked Cm^R, Ap^R, template for one-step recombineering	Addgene #45604
pKD4	*oriV*$_{R6K}$, FRT flanked Kn^R, Ap^R, template for one-step recombineering	Addgene #45605
pSIM6	*oriV*$_{pSC101ts}$, Lambda Red recombinase, *bla* (Ap^R)	Datta *et al.*, 2006 [18]
pWaaD	pBAD30, *waaD* under the control of P$_{BAD}$	Addgene #210448
pWaaID	pBAD30, *waaI* and *waaD* under the control of P$_{BAD}$	Addgene #210449
pWaaJ	pBAD30, *waaJ* under the control of P$_{BAD}$	Addgene #210450
pWaaK	pBAD30, *waaK* under the control of P$_{BAD}$	Addgene #210451
pWaaRK	pBAD30, *waaR* and *waaK* under the control of P$_{BAD}$	Addgene #210452
pWaaT	pBAD30, *waaT* under the control of P$_{BAD}$	Addgene #210453
pWaaW	pBAD30, *waaW* under the control of P$_{BAD}$	Addgene #210454

Supplementary Table 1. Strains and plasmids used in this study (continued).

Strain or plasmid	Description[a]	Source (reference)
pWaaTW-R1	pBAD30, *waaT* and *waaW* from R1 under the control of P_{BAD}	Addgene #210455
pWaaTW-R4	pBAD30, *waaT* and *waaW* from R4 under the control of P_{BAD}	Addgene #210456
pWaaV	pBAD30, *waaV* under the control of P_{BAD}	Addgene #210457
pWaaVL	pBAD30, *waaV* and *waaL* under the control of P_{BAD}	Addgene #210458
pWaaX	pBAD30, *waaX* under the control of P_{BAD}	Addgene #210459
pWaaOX	pBAD30, *waaO* and *waaX* under the control of P_{BAD}	This study
TP114	IncI2 conjugative plasmid, *aph*(3')-1 (Kn^R)	DSM-4246 (DSMZ)
TP114ΔKn::Cm	TP114 deletion mutant for the Kn resistance gene, replaced by the Cm resistance gene	This study
TP114Δ*pilV*::FLAG-*cat*	TP114 deletion mutant for the variable 3'-end of *pilV* gene replaced by a FLAG-tag, FRT flanked Cm^R	Allard *et al.* 2022 [8]
TP114Δshufflon::*pilVA-cat*	TP114 deletion mutant for the shufflon with *pilVA* fixed	Allard *et al.* 2022 [8]
TP114Δshufflon::*pilVA'-cat*	TP114 deletion mutant for the shufflon with *pilVA'* fixed	Allard *et al.* 2022 [8]
TP114Δshufflon::*pilVB-cat*	TP114 deletion mutant for the shufflon with *pilVB* fixed	Allard *et al.* 2022 [8]
TP114Δshufflon::*pilVB'-cat*	TP114 deletion mutant for the shufflon with *pilVB'* fixed	Allard *et al.* 2022 [8]
TP114Δshufflon::*pilVC-cat*	TP114 deletion mutant for the shufflon with *pilVC* fixed	Allard *et al.* 2022 [8]
TP114Δshufflon::*pilVC'-cat*	TP114 deletion mutant for the shufflon with *pilVC'* fixed	Allard *et al.* 2022 [8]
TP114Δshufflon::*pilVD-cat*	TP114 deletion mutant for the shufflon with *pilVD* fixed	Allard *et al.* 2022 [8]
TP114Δshufflon::*pilVD'-cat*	TP114 deletion mutant for the shufflon with *pilVD'* fixed	Allard *et al.* 2022 [8]
TP114Δshufflon::*pilVA-R64-cat*	TP114 deletion mutant for the shufflon with R64 *pilVA* fixed	This study
TP114Δshufflon::*pilVA'-R64-cat*	TP114 deletion mutant for the shufflon with R64 *pilVA'* fixed	This study
TP114Δshufflon::*pilVB-R64-cat*	TP114 deletion mutant for the shufflon with R64 *pilVB* fixed	This study

Supplementary Table 1. Strains and plasmids used in this study (continued).

Strain or plasmid	Description[a]	Source (reference)
TP114Δshufflon::*pilVB'-R64-cat*	TP114 deletion mutant for the shufflon with R64 *pilVB'* fixed	This study
TP114Δshufflon::*pilVC-R64-cat*	TP114 deletion mutant for the shufflon with R64 *pilVC* fixed	This study
TP114Δshufflon::*pilVC'-R64-cat*	TP114 deletion mutant for the shufflon with R64 *pilVC'* fixed	This study
TP114Δshufflon::*pilVD'-R64-cat*	TP114 deletion mutant for the shufflon with R64 *pilVD'* fixed	This study

[a] Ap^R, ampicillin; Cm^R, chloramphenicol; Kn^R, kanamycin; Nx^R, nalidixic acid; Sp^R, spectinomycin; DAP, diaminopimelic acid; ts, thermosensitive.

† Gift from Chris Whitfield, original from Max-Planck-Institute collection.

Supplementary Table 2: Oligonucleotides used in this study.

Context	Name	Sequence[a, b] (5'-3')	Template	Amplicon
BW25113ΔO antigen::Kn^R	oKn-F	atacctctattaatcaaactgagagccgcttatttcacagagattgcagcattacacgtc	pKD4	FRT flanked Kn^R
	oKn-R	ataaatagcttatccatgcttaaatgcttaacggctttatatggtccatatgaatatcctc		
	oBW1-F	gctcgtcacatcataggc	BW25113ΔO antigen	Screen O antigen deletion clones
	oBW1-R	cggcctggaatgttcgca		
TP114ΔKn::Cm	aph-III-pKD3-F	gtgcccgccgatgcgccaaccgcattcattaaagactaactagtaggctggagctgcttc	pKD3	FRT flanked Cm^R
	aph-III-pKD3-R	ataaaactgtctgcttacataaacagtaatacaaggggtgttgggaattagccatggtcc		
TP114 *pilV* variants derivatives	ocat-F	atgggaattagccatggtcc	pKD3	FRT flanked Cm^R
	opilV1-R	taaaaaatcactctgtagttgttctatcataagtgaatccgtgtaggctggagctgcttc		
TP114Δshufflon::*pilVA-R64-cat*	opilV22-F	cagtacaggggcgatactttcgtgccaatccggtcggtggaagacttctggttcgctcaa	R64	*pilVA*
	opilV22-R	ggaccatggctaattcccatttaagtttgatatccaaatactg		
TP114Δshufflon::*pilVA'-R64-cat*	opilV23-F	cagtacaggggcgatactttcgtgccaatccggtacgtgggggacaataggtggaaaact	R64	*pilVA'*
	opilV23-R	ggaccatggctaattcccatttaattgagcgttacacacgacgc		
TP114Δshufflon::*pilVB-R64-cat*	opilV24-F	cagtacaggggcgatactttcgtgccaatccggtacctggaaatcatcatcagcgtcgat	R64	*pilVB*
	opilV24-R	ggaccatggctaattcccatctatttcaagcaagtaatcttcataaagtagga		
TP114Δshufflon::*pilVB'-R64-cat*	opilV25-F	cagtacaggggcgatactttcgtgccaatccggtacctggagaaaggtaggatctggtga	R64	*pilVB'*
	opilV25-R	ggaccatggctaattcccatttattggcaaatggcatatacagttattgaac		
TP114Δshufflon::*pilVC-R64-cat*	opilV26-F	cagtacaggggcgatactttcgtgccaatccggtacctggggcgctcctaaaattcaatt	R64	*pilVC*
	opilV26-R	ggaccatggctaattcccatttaagctccagcaccaggaaga		
TP114Δshufflon::*pilVC'-R64-cat*	opilV27-F	cagtacaggggcgatactttcgtgccaatccggtcggtggtcaggggtaataaaattaa	R64	*pilVC'*
	opilV27-R	ggaccatggctaattcccatttaattaaaggggcaacagtaggca		
TP114Δshufflon::*pilVD'-R64-cat*	opilV28-F	cagtacaggggcgatactttcgtgccaatccggtacttggcgtaaaagcaattctggtag	R64	*pilVD'*
	opilV28-R	ggaccatggctaattcccattcagttctgacacgcgacga		
pWaa plasmid series	opBAD30-F	gcatgcaagcttggctgttttg	pBAD30	pBAD30 backbone
	opBAD30-R	ttttgcctcctagagctcgaattcgctagccc		

Supplementary Table 2: Oligonucleotides used in this study (continued).

Context	Name	Sequence[a, b] (5'-3')	Template	Amplicon
pWaaD	owaa1-F	tcgagctctaggaggcaaaaatggttgataaaataatatttacggtt	F653	*waaD*
	owaa1-R	aaacagccaagcttgcatgcttaaacaaaccaattatgaataacct		
pWaaID	owaa2-F	tcgagctctaggaggcaaaaatgtctcaactcaatgatag	F653	*waaI*
	owaa2-R	accttaaatctttagaagcatt		
	owaa3-F	tgcttctaaagatttaaggttatacgagatggttgataaa	F653	*waaD*
	owaa1-R	aaacagccaagcttgcatgcttaaacaaaccaattatgaataacct		
pWaaJ	owaa4-F	tcgagctctaggaggcaaaaatgaaattggattttaaacatcttact	F653	*waaJ*
	owaa4-R	aaacagccaagcttgcatgcttaacctttcataacattatatttaattgc		
pWaaK	owaa5-F	tcgagctctaggaggcaaaaatgattaaaaaaaataatatttaccgtca	F632	*waaK*
	owaa5-R	aaacagccaagcttgcatgcttaaccaaaccagtcttgtatt		
pWaaRK	owaa6-R	tcgagctctaggaggcaaaagtgaactcatttcctgccat	F632	*waaR*
	owaa6-F	gttaaaccagttaaatgttatttacg		
	owaa7-F	taacatttaactggtttaacgagttggctaataatgattaa	F632	*waaK*
	owaa5-R	aaacagccaagcttgcatgcttaaccaaaccagtcttgtatt		
pWaaRK	owaa6-R	tcgagctctaggaggcaaaagtgaactcatttcctgccat	F632	*waaR*
	owaa6-F	gttaaaccagttaaatgttatttacg		
	owaa7-F	taacatttaactggtttaacgagttggctaataatgattaa	F632	*waaK*
	owaa5-R	aaacagccaagcttgcatgcttaaccaaaccagtcttgtatt		
pWaaT	owaa8-F	tcgagctctaggaggcaaaaatgaatgaatttataaaagaacggttttcg	Nissle 1917	*waaT*
	owaa8-R	aaacagccaagcttgcatgcttatttcttaagcttgtacttaattaatgaa		
pWaaW	owaa9-F	tcgagctctaggaggcaaaaatggatttattagctgagagtatt	Nissle 1917	*waaW*
	owaa9-R	aaacagccaagcttgcatgcttattgcccaaatagttttctttta		
pWaaTW-R1	owaa8-F	tcgagctctaggaggcaaaaatgaatgaatttataaaagaacggttttcg	Nissle 1917	*waaT*
	owaa7-R	aagagtaatttatttcttaagcttgt		
	owaa10-F	acaagcttaagaaataaattactcttatggatttattagctgagag	Nissle 1917	*waaW*
	owaa9-R	aaacagccaagcttgcatgcttattgcccaaatagttttctttta		
pWaaV	owaa11-F	tcgagctctaggaggcaaaaatgagcaatgattacccttt	Nissle 1917	*waaV*
	owaa11-R	aaacagccaagcttgcatgcctaacgtttattctttttctatttacc		
pWaaVL	owaa11-F	tcgagctctaggaggcaaaaatgagcaatgattacccttt	Nissle 1917	*waaVL*
	owaa10-R	aaacagccaagcttgcatgcttacttatctaataaacattgg		

Supplementary Table 2: Oligonucleotides used in this study (continued).

Context	Name	Sequence[a, b] (5'-3')	Template	Amplicon
pWaaX	owaa12-F	tcgagctctaggaggcaaaaatgaacttgcccatttatattgt	F2513	*waaX*
	owaa12-R	aaacagccaagcttgcatgctcatttcaaaagagaaaaaaaagcc		
pWaaOX	owaa13-F	tcgagctctaggaggcaaaaatgagtgcccactattttaa	F2513	*waaO*
	owaa13-R	taaatgggcaagttcattaattaacttttctcaatttcattt		
	owaa14-F	aaatgaaattgagaaaagttaattaatgaacttgcccattta	F2513	*waaX*
	owaa12-R	aaacagccaagcttgcatgctcatttcaaaagagaaaaaaaagcc		
pWaaTW-R4	owaa8-F	tcgagctctaggaggcaaaaatgaatgaatttataaaagaacggttttcg	F2513	*waaT*
	owaa14-R	ttccgttttgactgtgtggtttatttcttaagcttgtacttaatt		
	owaa15-F	agtacaagcttaagaaataaaccacacagtcaaaacggaa	F2513	*waaW*
	owaa15-R	aaacagccaagcttgcatgcatctctgggtgattaatcttaataatta		

[a]Underline represent binding nucleotides

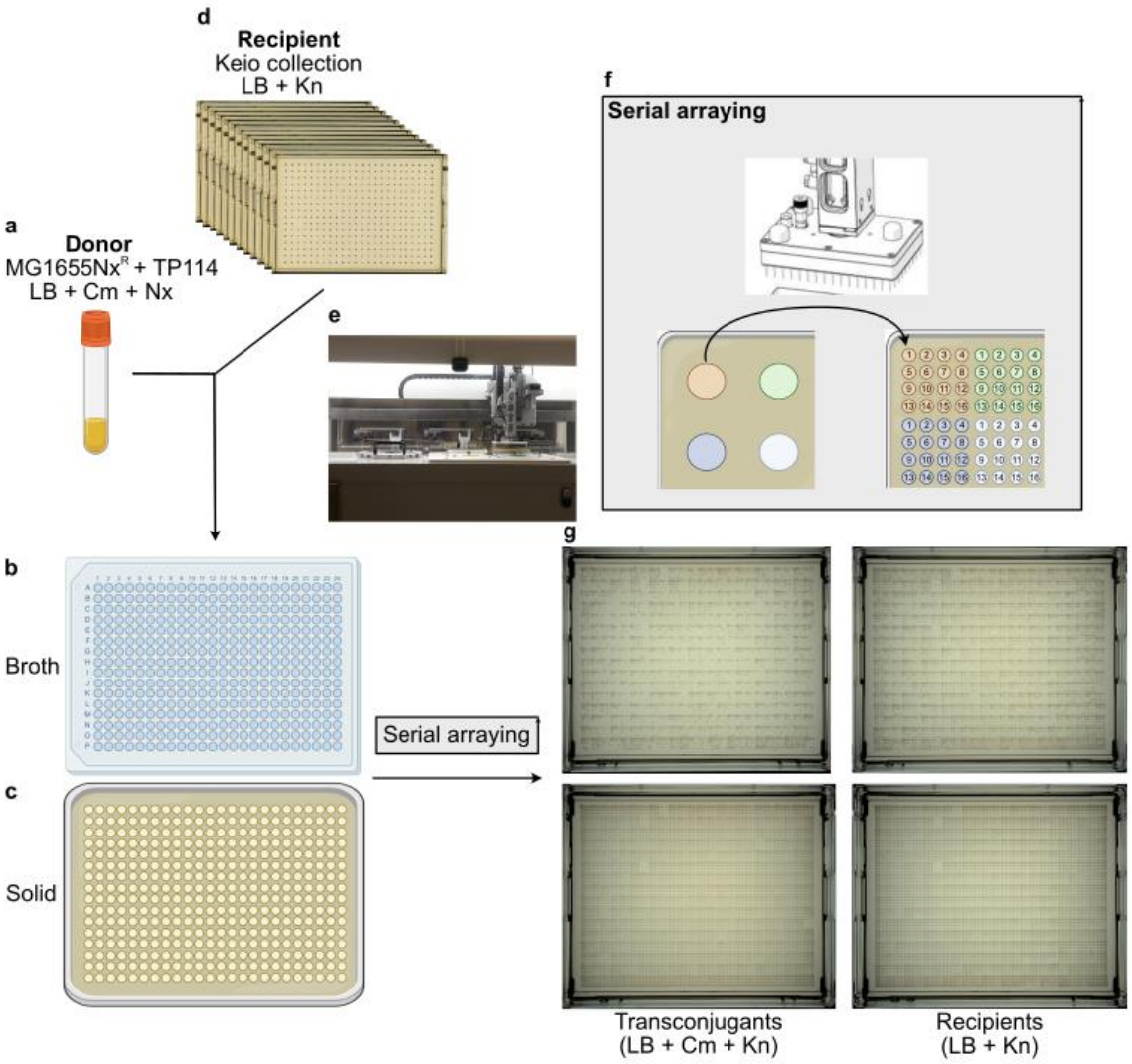

Supplementary Figure 1 | High throughput conjugation assays.

Our protocol allows the transfer of a conjugative plasmid from a donor strain towards the 3985 single-gene deletion mutants from the Keio collection, and the 141 small RNA/small protein deletion mutants. The determination of a conjugation score is then calculated for every possible mutant. **a**, The donor bacterium (*E. coli* MG1655Nx^{R} + TP114) is grown overnight at 37°C in LB containing chloramphenicol (selective marker of TP114) and nalidixic acid, normalized to an OD600nm of 0.1, and transferred into 384-well mating plates (**b**, broth mating) or onto LB-agar mating plates (**c**, solid mating). **d**, At the same time, the deletion mutants are grown overnight at 37°C in LB with kanamycin (selection marker of the mutants) in 384-well plates and transferred to the 384-well and LB-agar mating

plates using the Singer Rotor HDA (**e**). **f**, After 6h of conjugation at 37°C, mating plates were replicated using the Singer Rotor HDA on two selection plates, containing kanamycin and chloramphenicol to select the transconjugants (deletion mutants that have acquired TP114) or kanamycin only to select recipient bacteria. To do so, each conjugation was replicated 16 times sequentially to create a serial dilution array to be able to assess the transfer rate for each mutant. Plates are then incubated at 37°C overnight before being imaged (**g**), and the growth of each mutant is converted into a density value. Finally, a ratio between transconjugant density and recipient density is made to determine the conjugation score of each mutant.

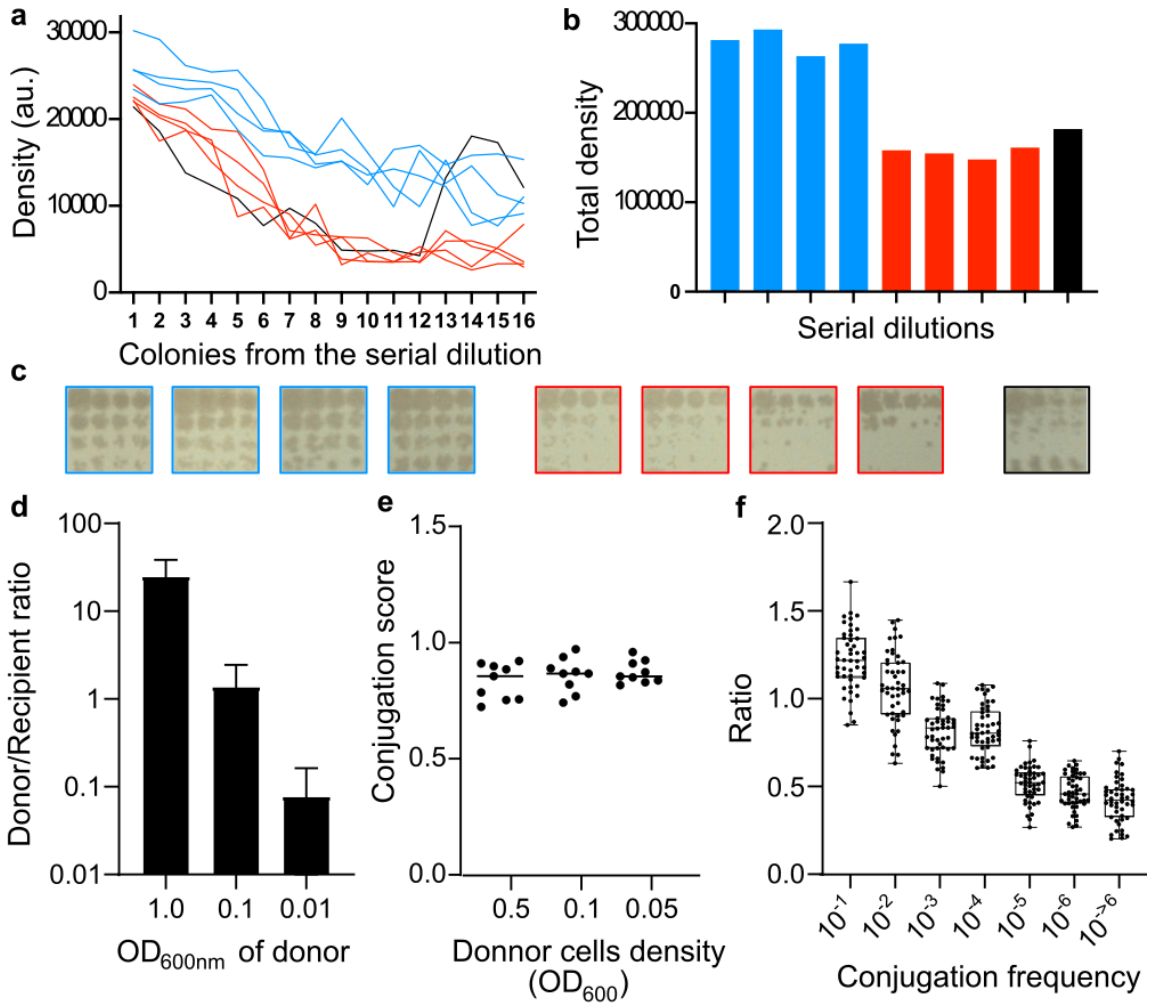

Supplementary Figure 2 | High-throughput screen validation. To determine the linear range of the serial dilution from our high-throughput assay, we randomly selected four high-density wells (blue), four low-density wells (red) and one well with colonies at later dilution spots from a recipient plate of the screen (black) for liquid mating. We then measured the density of individual dilution spots in FIJI. (**a**) Density of the 16 individual dilution spots from the 9 wells. (**b**) Total density of the 9 wells. (**c**) Image of the selected wells. (**d**) To measure the ratio of donor to recipient cells in high-throughput conjugation assays, the donor cells harboring conjugative plasmid TP114 were resuspended at an OD_{600nm} of 1.0, 0.1 or 0.01, and 50 µL of these suspensions were added to a 384-well plate. The recipient strain *E. coli* BW25113Δ*yejO* – a deletion mutant of a pseudogene in *E. coli* K-12, was then pinned into the 384-well plates. CFUs were then counted directly from these wells (at T=0 of conjugation). Each bar shows the average ratio for 8 wells. (**e**) Donor cells harboring TP114 were resuspended at various OD_{600nm} and mixed

with the *E. coli* BW25113Δ*yejO* recipient strain to vary donor to recipient ratios. After a 6h conjugation time, transconjugants (Kn and Cm) and recipients (Kn) were selected and the transfer rate was measured as described in the manuscript. (**f**) TP114 variants with different transfer rates were used in the standard manual conjugation assay or high-throughput screening approach. The TP114 variants were hosted in *E. coli* MG1655Nx^{R} as the donor and were transferred to the *E. coli* BW25113Δ*yejO* recipient strain in broth using the high-throughput conjugation assay. The results suggest that conjugation scores track relatively well with manual transfer rates with a detection limit around 10^{-5}.

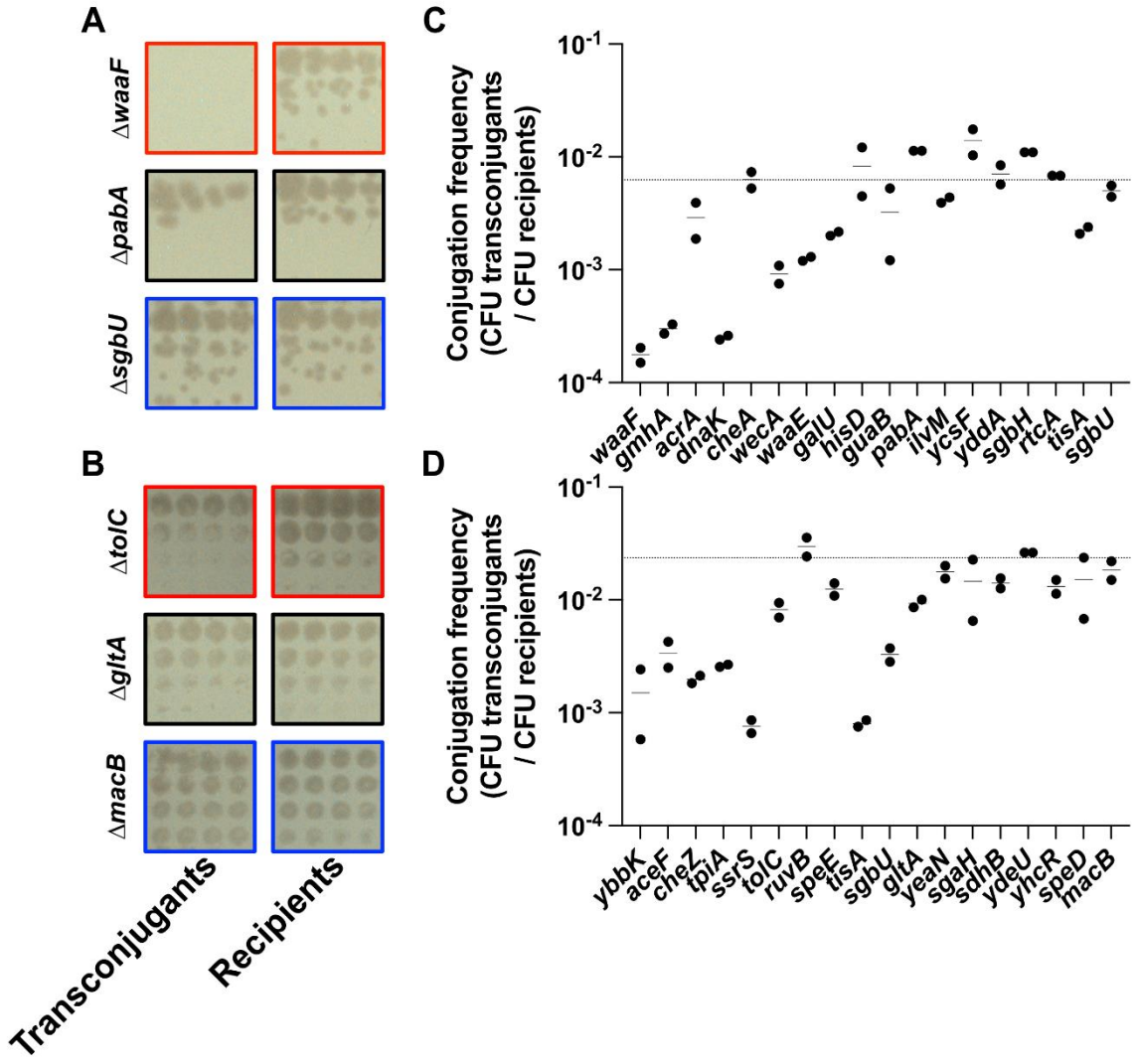

Supplementary Figure 3 | Transconjugants and recipients growth after high-throughput conjugation assays.

Examples of the serial dilution growth after high-throughput conjugation assays in broth (**a**) and on a solid support (**b**). Each square represents the sequential replicate (16 in total) to create a serial dilution array and allow us to assess the transfer rate of each mutant. Transconjugants grew on LB plates containing Kn (selection marker of the Keio collection) and Cm (selection marker of the conjugative plasmid TP114), whereas recipients grew on LB plates containing Kn only. Deletion mutants were selected according to their low, medium, and high conjugation scores. Conjugation efficiency of selected genes in broth (**c**) or on solid (**d**) using a standard manual conjugation assay to validate the results of the screen.

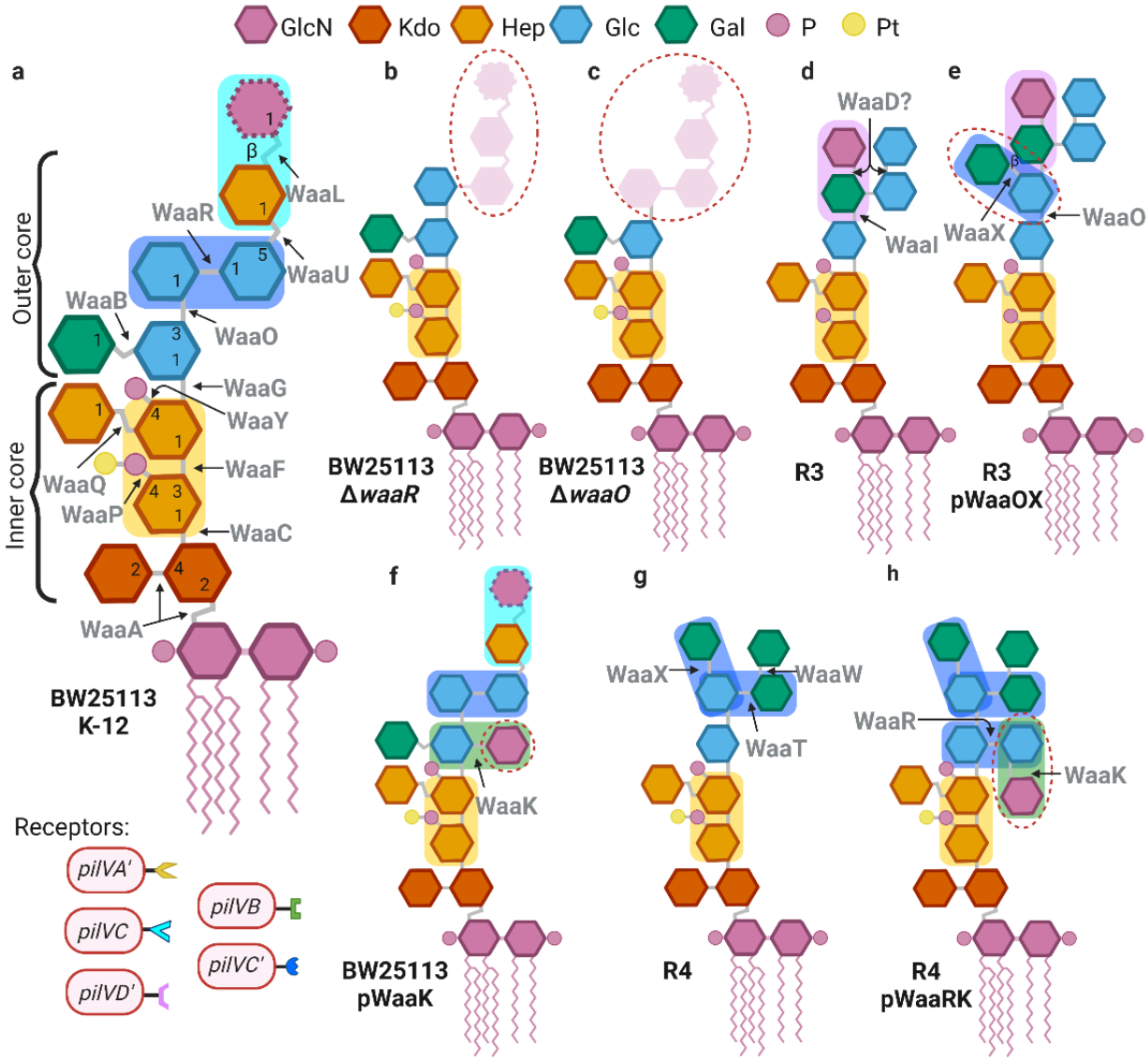

Supplementary Figure 4 | Comparison of LPS from *E. coli* strains. a, The LPS structure of *E. coli* BW25113 with a K-12 core-OS is shown. The genes whose products catalyze the formation of each linkage are shown in gray. **b-h**, The expected LPS structures of some knockout[52] and knock-in mutants used in this study. The residues that are lost are depicted in pink and they are circled in red dotted lines. The LPS structure of *E. coli* R4 is also shown (**g**) and the expected LPS structure of *E. coli* R4 transformed with pWaaRK (**h**). All glycoses are in the *α*-anomeric configuration unless stated otherwise. The specific receptor structures for the different PilV adhesins in the LPS molecules are indicated in colored rectangles. Abbreviations of monosaccharide residues: GlcN, glucosamine; Kdo,

2-keto-3-deoxyoctulosonic acid (3-deoxy-D-*manno*-octulosonic acid); Hep, L-*glycero*-D-*manno*-heptose; Glc, glucose; Gal, galactose; P, phosphate; Pt, pyrophosphoethanolamine. Created in BioRender.com.

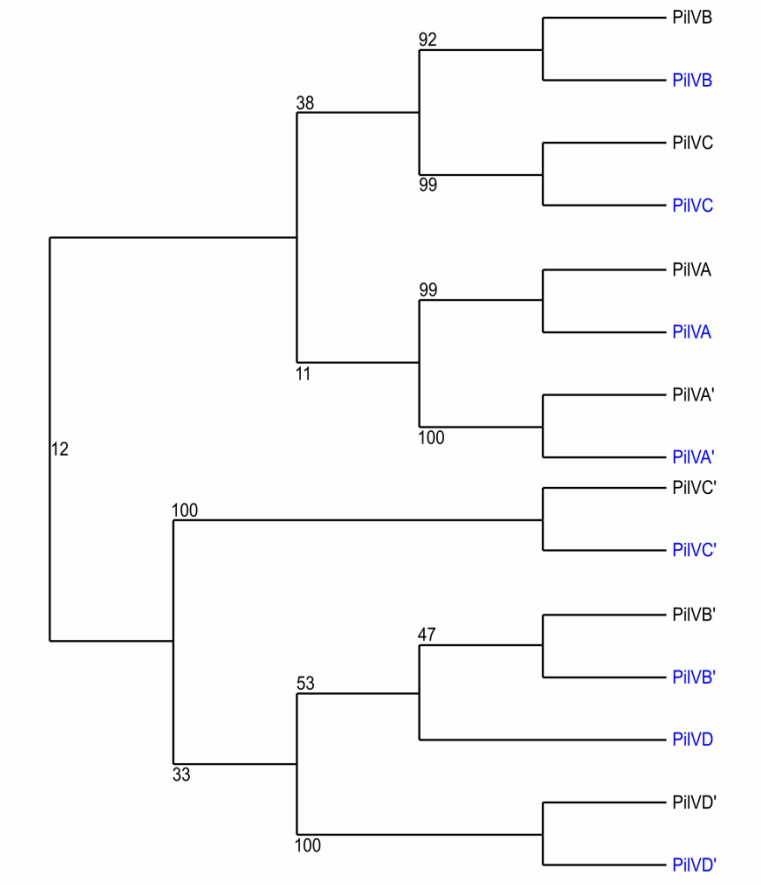

Supplementary Figure 5 | Phylogenetic tree of PilV adhesins from conjugative plasmids R64 and TP114.

Phylogenetic tree showing the relationship among the variable C-terminal minor adhesins (PilV) amino acid sequences of conjugative plasmids R64 (AP005147.1) and TP114 (MF521836.2). All analyzed C-terminal adhesins from R64 are paired with their homologue in TP114. The PilVD variant from TP114 seems to have probably evolved from PilVB' adhesin. The tree was generated by maximum likelihood analysis in SeaView 5.0.4 software. Bootstrap analysis was performed on 1000 trees and the values are provided on the branch nodes. TP114 adhesins are indicated in blue.

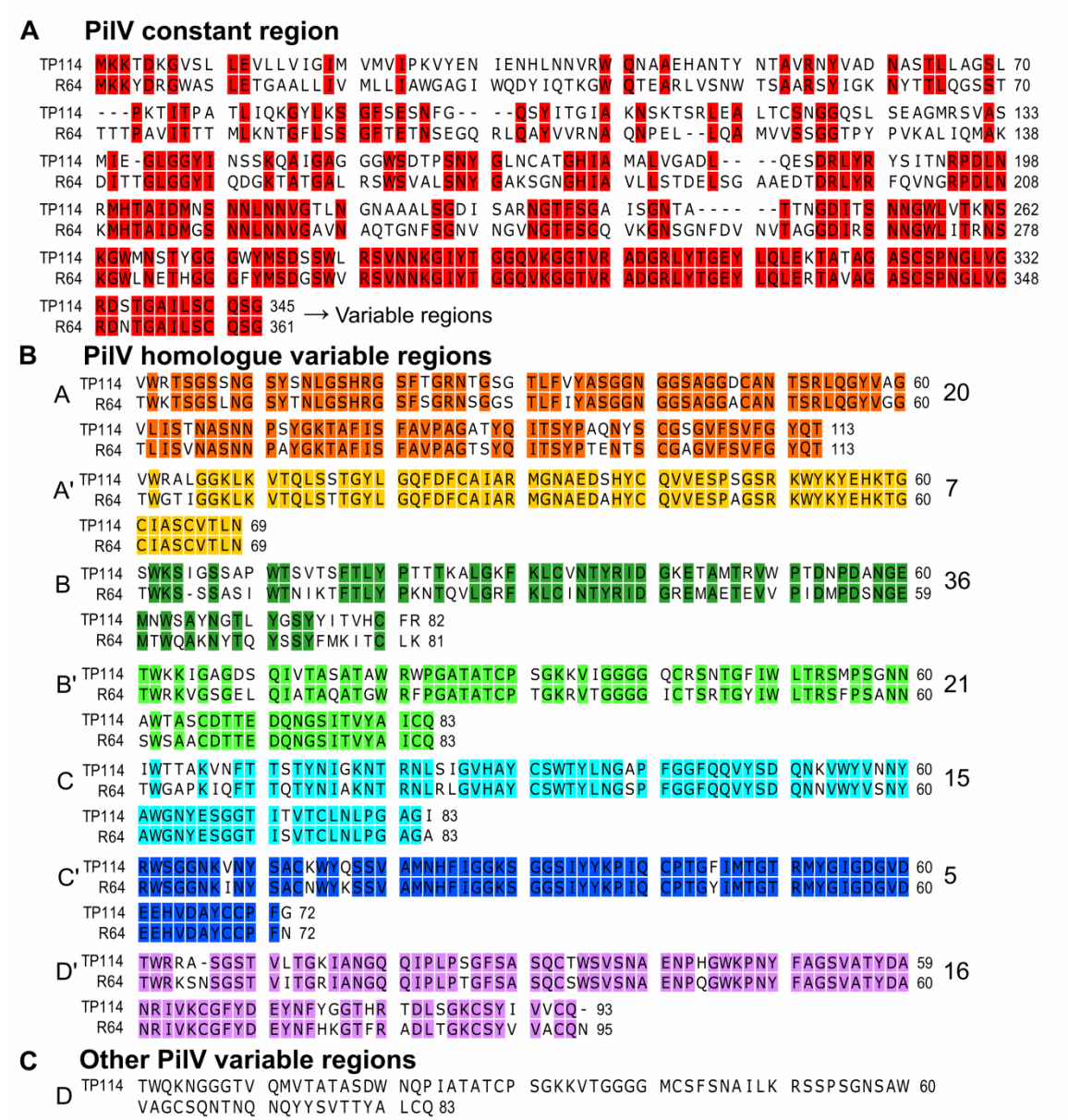

Supplementary Figure 6 | Sequence comparison of PilV adhesins from conjugative plasmids R64 and TP114.

Amino acid sequences of constant and variable regions from adhesins displayed by conjugative plasmids R64 (AP005147.1) and TP114 (MF521836.2). Sequence alignments were performed with CLC Main Workbench. The amino acid residues conserved between each homologue are indicated in color. The number of mismatched amino acids is indicated on the right of the alignments.

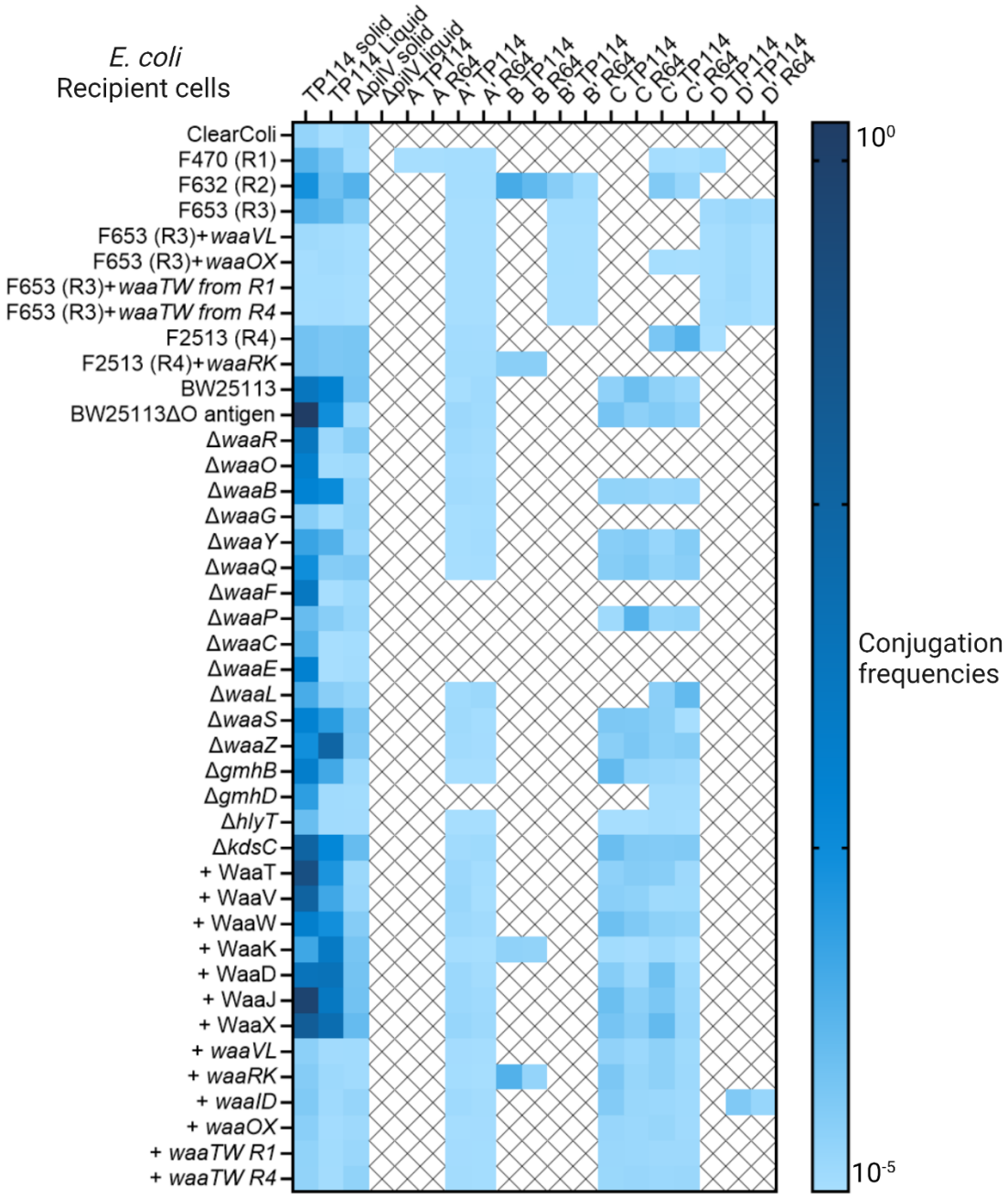

Supplementary Figure 7 | Conjugation transfer rates of TP114 derivatives.

Heat map illustrating the transfer rates of wild-type TP114 along with all the derived plasmids expressing only one variant of PilV either from TP114 or R64 against various *E. coli* recipient cells. All conjugations were performed in biological triplicate with *E. coli* Nissle 1917Δ*dapA* as the donor strain (n=3). Cross marks indicate conjugation frequencies below the detection limit of the experiment (1 x 10^{-8}) in most cases. However, to avoid false positive results, we considered that

the conjugation results underneath 5.9×10^{-5} were not significant and were identified with a cross mark as well.

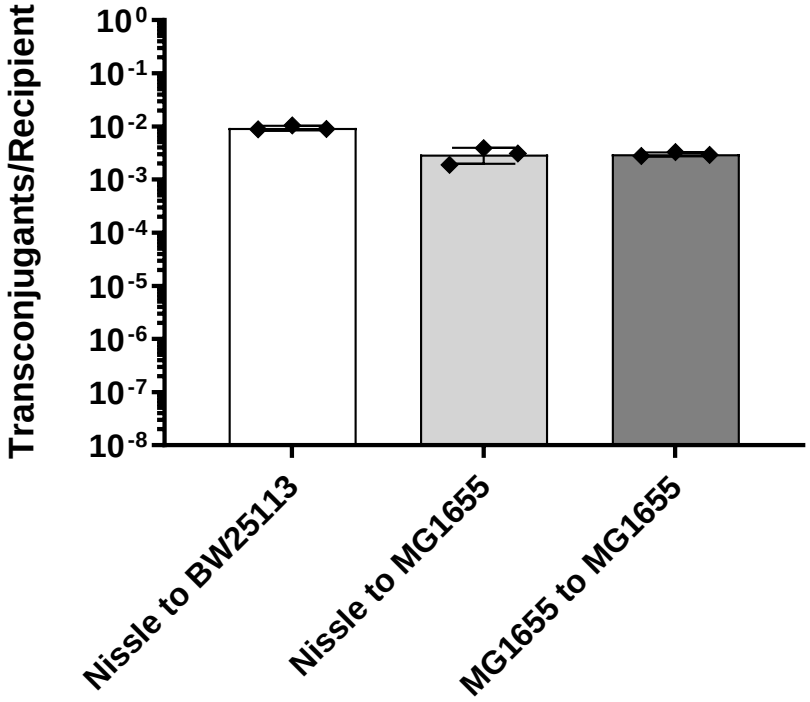

Supplementary Figure 8 | Impact of different donor and recipient strain combinations on the transfer of conjugative plasmid TP114.

Three different combinations of donor and recipient strains were assayed in LB broth for 2-hour at 37ºC before plating on a appropriate selective medium and counting the number of CFU to obtain transfer rates (n=3).

Supplementary References.

1. Browning, D. F. *et al.* Laboratory adapted *Escherichia coli* K-12 becomes a pathogen of *Caenorhabditis elegans* upon restoration of O antigen biosynthesis. *Mol. Microbiol.* **87**, 939–950 (2013).
2. Whitfield, C. & Valvano, M. A. Biosynthesis and expression of cell-surface polysaccharides in Gram-negative bacteria. *Adv. Microb. Physiol.* **35**, 135–246 (1993).
3. Liu, B. *et al.* Structure and genetics of *Escherichia coli* O antigens. *FEMS Microbiol. Rev.* **44**, 655–683 (2020).
4. Heinrichs, D. E., Yethon, J. A. & Whitfield, C. Molecular basis for structural diversity in the core regions of the lipopolysaccharides of *Escherichia coli* and *Salmonella enterica*. *Mol. Microbiol.* **30**, 221–232 (1998).
5. Feldman, M. F. *et al.* The activity of a putative polyisoprenol-linked sugar translocase (Wzx) involved in *Escherichia coli* O antigen assembly is independent of the chemical structure of the O repeat. *J. Biol. Chem.* **274**, 35129–35138 (1999).
6. Stevenson, G. *et al.* Structure of the O antigen of *Escherichia coli* K-12 and the sequence of its *rfb* gene cluster. *J. Bacteriol.* **176**, 4144–4156 (1994).
7. Mamat, U. *et al.* Endotoxin-free protein production—ClearColi^{TM} technology. *Nat. Methods* **10**, 916 (2013).
8. Allard, N., Neil, K., Grenier, F. & Rodrigue, S. The type IV pilus of plasmid TP114 displays adhesins conferring conjugation specificity and is important for DNA transfer in the mouse gut microbiota. *Microbiol. Spectr.* **10**, e0230321 (2022).
9. Ishiwa, A. & Komano, T. PilV adhesins of plasmid R64 thin pili specifically bind to the lipopolysaccharides of recipient cells. *J. Mol. Biol.* **343**, 615–625 (2004).
10. Ishiwa, A. & Komano, T. Thin pilus PilV adhesins of plasmid R64 recognize specific structures of the lipopolysaccharide molecules of recipient cells. *J. Bacteriol.* **185**, 5192–5199 (2003).
11. Cress, B. F., Linhardt, R. J. & Koffas, M. A. G. Draft genome sequence of *Escherichia coli* strain Nissle 1917 (serovar O6:K5:H1). *Genome Announc.* **1**, e0004713 (2013).
12. Neil, K., Allard, N., Grenier, F., Burrus, V. & Rodrigue, S. Highly efficient gene transfer in the mouse gut microbiota is enabled by the IncI2 conjugative plasmid TP114. *Commun. Biol.* **3**, 523 (2020).
13. Ceccarelli, D., Daccord, A., René, M. & Burrus, V. Identification of the origin of transfer (*oriT*) and a new gene required for mobilization of the SXT/R391 family of integrating conjugative elements. *J. Bacteriol.* **190**, 5328–5338 (2008).
14. Baba, T. *et al.* Construction of *Escherichia coli* K-12 in-frame, single-gene knockout mutants: The Keio collection. *Mol. Syst. Biol.* **2**, 2006.0008 (2006).
15. Tsang, R. S. *et al.* A murine monoclonal antibody specific for the outer core oligosaccharide of *Salmonella* lipopolysaccharide. *Infect. Immun.* **55**, 211–

216 (1987).
16. Hämmerling, G., Lüderitz, O., Westphal, O. & Mäkelä, P. H. Structural investigations on the core polysaccharide of *Escherichia coli* O100. *Eur J Biochem* **22**, 331–344 (1971).
17. Guzman, L. M., Belin, D., Carson, M. J. & Beckwith, J. Tight regulation, modulation, and high-level expression by vectors containing the arabinose PBAD promoter. *J. Bacteriol.* **177**, 4121–4130 (1995).
18. Datta, S., Costantino, N. & Court, D. L. A set of recombineering plasmids for Gram-negative bacteria. *Gene.* **379**, 109–115 (2006).
19. Nakao, R., Ramstedt, M., Wai, S. N. & Uhlin, B. E. Enhanced biofilm formation by *Escherichia coli* LPS mutants defective in Hep biosynthesis. *PLoS One* **7**, e51241 (2012).